# LIDAR SCAN MATCHING WITH PPP-RTK FOR 3D FARM MAPPING

Masafumi Nakagawa[1], Sayaka Yokoyama[1], Tomohiro Ozeki[2], Nobuaki Kubo[2]
Hiromune Namie[3], Masashi Yoshida[4], Yoshihiro Iwaki[5]
[1]Shibaura Institute of Technology, 3-7-5, Toyosu, Koto-ku, Tokyo 135-8548, Japan,
Email: mnaka@shibaura-it.ac.jp
[2]Tokyo University of Marine Science and Technology
[3]National Defense Academy
[4]Salesian Polytechnic Mechanical and Electronic Engineering
[5]Iwaki Farm

**KEY WORDS:** Scan matching, Multilayer LiDAR, PPP-RTK, Mobile mapping, Smart agriculture

**ABSTRACT:** In various advanced agriculture activities called smart agriculture, we focus on three-dimensional measurements for farm mapping and machine control. We also focus on precise point positioning real-time kinematic systems, such as Global Navigation Satellite System (GNSS) positioning with submeter-level augmentation services (SLAS), centimeter-level augmentation services (CLAS), and multi-GNSS advanced demonstration tool for orbit and clock analysis (MADOCA) to improve the efficiency of precise positioning using the Quasi-Zenith Satellite System. In our study, we selected a farm as an experiment area to acquire point clouds and position data of cultivation works before sowing soybeans. We used a low-price light detection and ranging device with a multifrequency GNSS. Through our experiment, we evaluated the positioning performance of SLAS, CLAS, and MADOCA for point cloud acquisition. Moreover, we confirmed that our methodology can reconstruct point clouds from a tractor.

## 1. INTRODUCTION

In the agriculture field, many farms have begun activities including satellite remote sensing, aerial remote sensing using unmanned aerial vehicles, Internet of Things (IoT) devices, and autonomous farm machines to improve the cost and efficiency of farming works. Various advanced agricultural activities are covered in smart agriculture and IoT applications for smart agriculture can be classified into seven categories: smart monitoring, smart water management, agrochemicals applications, disease management, smart harvesting, supply chain management, and smart agricultural practices (Friha et al., 2021). In addition, smart agriculture uses various types of agricultural sensors such as location-based sensors, optical sensors, and temperature-based sensors (Maddikunta et al., 2021). Thus, we focus on the three-dimensional (3D) measurement and mapping for farm and sensor data management and machine control. Autonomous farm machines mainly use real-time kinematic Global Navigation Satellite System (RTK-GNSS) positioning data, thus, RTK-GNSS positioning is required for precise position data acquisition for agriculture automation. In rural areas, however, a base station and stable communication environments should be prepared to achieve precise and continuous RTK-GNSS positioning. Therefore, we focus on submeter-level augmentation services (SLAS), centimeter-level augmentation services (CLAS), and multi-GNSS advanced demonstration tool for orbit and clock analysis (MADOCA) to improve the efficiency of precise positioning using a Quasi-Zenith Satellite System (QZSS). After the official operation of the four quasi-zenith satellites, L6 centimeter-level augmentation signal (L6D-CLAS), L6 multi-GNSS advanced demonstration tool for orbit and clock analysis signal (L6E-MADOCA), and a QZS safety confirmation service (Q-ANPI) were implemented (Namie et al., 2021).
We also focus on 3D measurement with CLAS from farming machines to acquire point clouds in farming works. We have proposed a scan matching for multilayer light detection and ranging (LiDAR) (i.e., 3D LiDAR) data registration with RTK-GNSS positioning and geometric constraints (Nakagawa et al., 2020). Based on this approach, we apply CLAS as precise point positioning-RTK (PPP-RTK) with LiDAR for 3D measurement. In this study, we selected a farm as an experiment area to acquire point clouds and position data of cultivation works before sowing soybeans. Through our experiment with low-price LiDAR and multifrequency GNSS devices, we evaluate the positioning performance of SLAS, CLAS, and MADOCA for point cloud acquisition. Moreover, we confirm that our methodology can reconstruct point clouds from a tractor and tractors' activities.

## 2. METHODOLOGY

Mobile mapping systems generally use LiDAR, GNSS positioning, and inertial measurement unit (IMU) data to generate point clouds. Alternatively, our methodology generates point clouds without IMU data. Our proposed methodology consists of synchronized data acquisition, initial point cloud registration, fine registration, and tractor activity estimation, as shown in Figure 1.

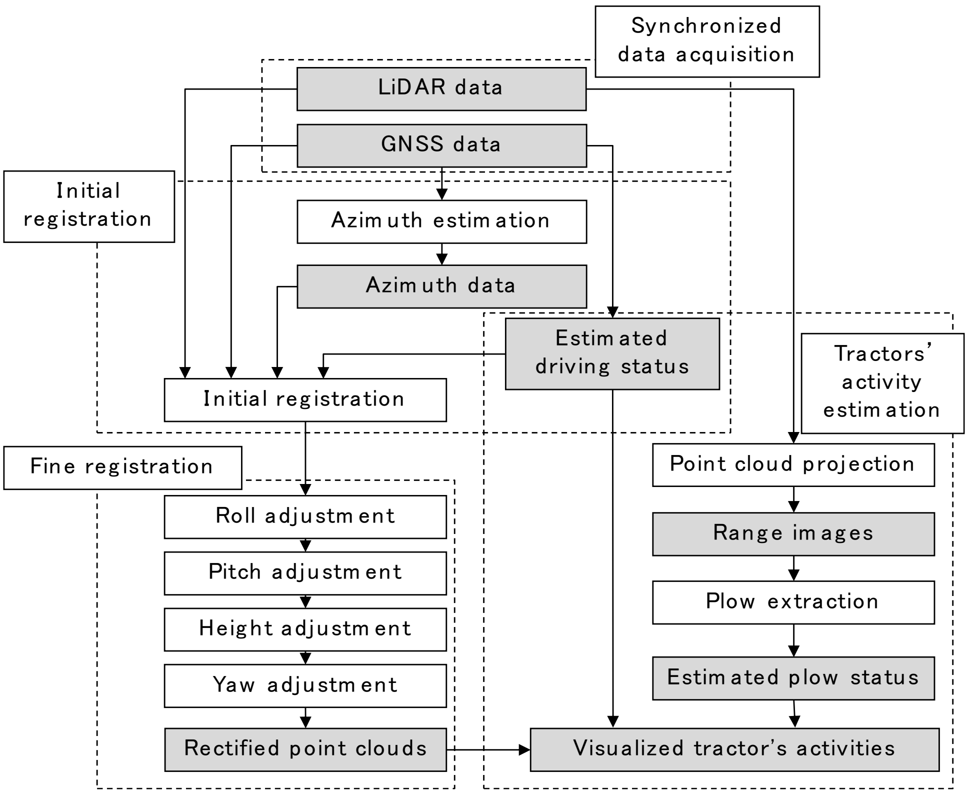


Figure 1. Proposed methodology

First, synchronized LiDAR and GNSS data were acquired. The use of a multilayer LiDAR and RTK-GNSS device is required for our methodology. Moreover, point clouds obtained by LiDAR should have a timestamp for each scanning. When a LiDAR device is mounted on a platform without a direct connection to RTK-GNSS devices, the device should have an additional GNSS antenna for precise timing.

Second, in the initial point cloud registration, the driving status and azimuth data were estimated from acquired GNSS positioning data. Driving status, such as stopping and running, can be estimated from differences in temporal GNSS position data. When RTK-GNSS positioning is applied for driving status estimation, running status can be distinguished from stopping status with a threshold value such as 3 cm/sec, because the positioning accuracy is approximately within 3 cm. Next, azimuth data were estimated from temporal GNSS positioning data during the operation of the tractor as a driving direction for initial point cloud registration before LiDAR scan matching processing. After the azimuth estimation, the LiDAR position is estimated using the azimuth data and offset distances between the GNSS antenna and LiDAR. Then, point clouds are integrated using estimated azimuth and LiDAR position data as an initial registration, as shown in Figure 2.

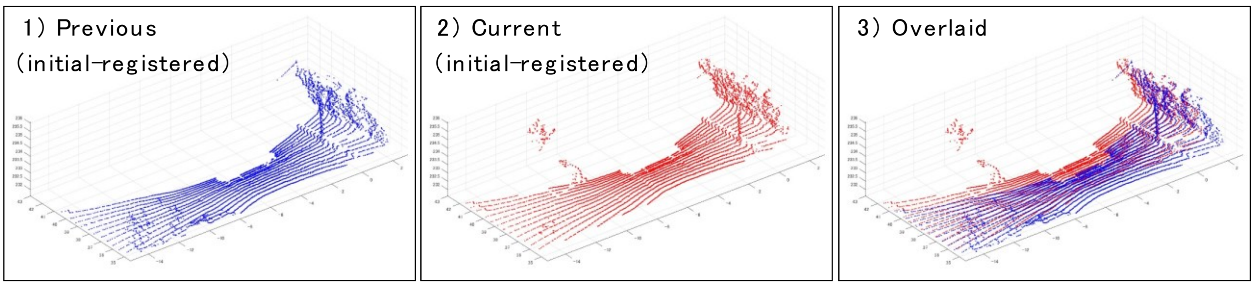


Figure 2. Initial point cloud registration

Third, in the fine registration, the initial point clouds are refined through orientation adjustment steps consisting of roll, pitch, height, and yaw adjustments. In our methodology, rotation data are estimated from LiDAR scan matching instead of IMU data acquisition. Moreover, in mobile mapping with low-price LiDAR and RTK-GNSS, horizontal position data obtained with GNSS are enough to be used as position data for point cloud registration. However, the

height data are not enough to be used for point cloud registration. Thus, roll, pitch, yaw, and height are adjusted.
In LiDAR scan matching processing, first, dense point clouds are generated from base point clouds, as shown in Figure 3. When dense point clouds are used for LiDAR scan matching, we usually apply an approach to find the closest points such as the iterative closest point (ICP) algorithm. However, when sparse point clouds are used for LiDAR scan matching, the ICP finds matched points with high scores even though no corresponded points exist. Thus, in our methodology, we apply an interpolation of base point clouds to prepare corresponded points. Next, point clouds are divided into horizontal and vertical surfaces, as shown in Figure 4. Point clouds of horizontal surfaces are used for roll and pitch angle adjustment processing, while point clouds of vertical surfaces are used for yaw angle adjustment processing. When no vertical objects exist, azimuth data estimated from GNSS data are directly used as yaw data without yaw adjustment processing.

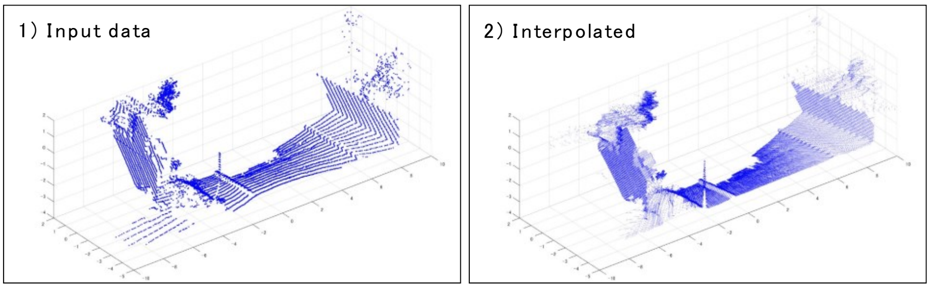


Figure 3. Point cloud interpolation for fine registration

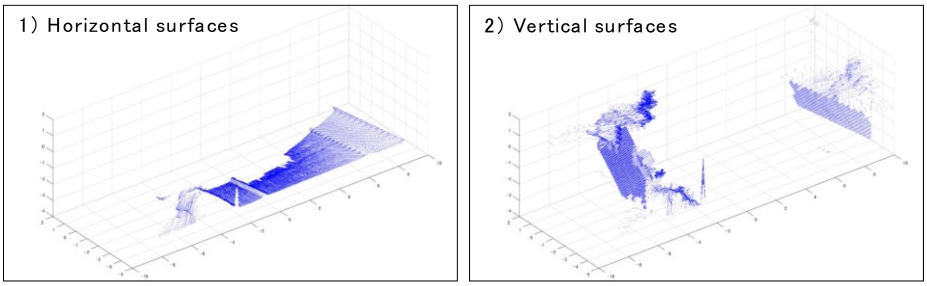


Figure 4. Point cloud division for fine registration

Fourth, the tractor's activities are reconstructed with estimated driving and plow status onto rectified point clouds after status estimation. The plow status is estimated using temporal range images generated from LiDAR data. When a LiDAR device is mounted on a tractor at a position where a plow is scanned, the plow's activity can be measured using LiDAR. Figure 5 shows an example of plow up and down. The upper image a shows a depth image at a plow-up scene. The horizontal axis indicates scanning direction, and the vertical axis indicates scanning channels. The center image b shows a depth image at a scene plow-down. The bottom image c shows a temporal graph of plow positions. The horizontal axis indicates scenes, and the vertical axis indicates distance values from the LiDAR device to the plow.

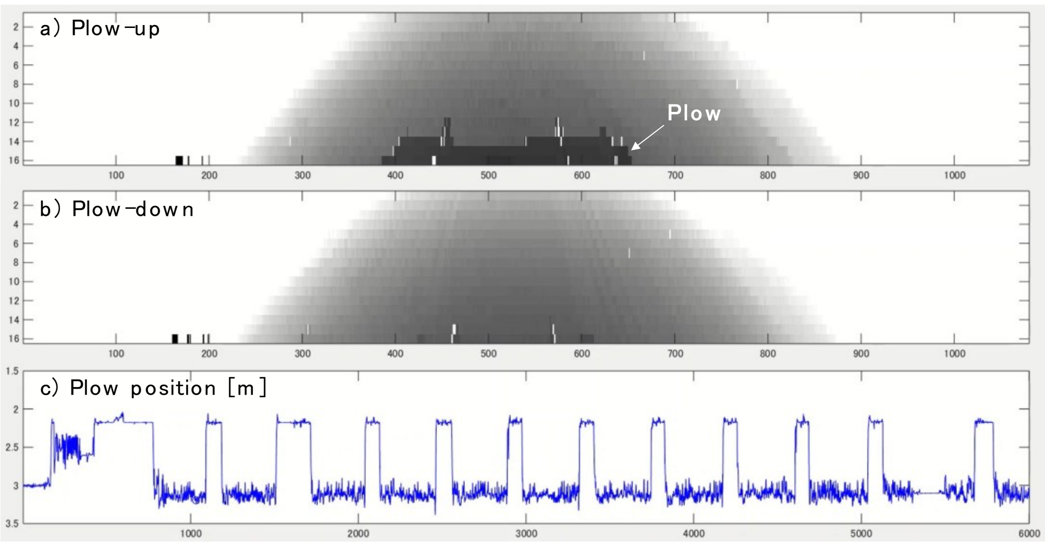

Figure 5. An example of plow up and down

## 3. EXPERIMENTS

We selected the Iwaki farm (Otawara, Tochigi, Japan) as an experimental area to evaluate the 3D measurement methodology using farming machines in farming works. LiDAR and GNSS positioning data were acquired during cultivation works before sowing soybeans. We used low-price multilayer LiDAR and multifrequency GNSS devices. The LiDAR device (VLP-16, Velodyne) was mounted on a tractor (MR70, Kubota) in a diagonal down-backward manner to acquire point clouds of fields during cultivation works, as shown in Figure 6. The GNSS antenna (GPS-703-GGG-HV, NovAtel) was mounted on the bonnet of the tractor. After our preliminary experiments, we selected the bonnet as a better position for stable GNSS signals receiving. We acquired SLAS data with ZED-F9P (u-blox), CLAS data with AsteRx4 (Septentrio), and MADOCA data with Owl-TypeB (LiGHTHOUSE). We also acquired RTK-GNSS positioning data with ZED-F9P (u-blox) as the reference data. In our experiments, we evaluated the positioning performance of SLAS, CLAS, and MADOCA. Moreover, we used CLAS data for point cloud generation to evaluate our methodology. Then, we represented the tractor's activities with estimated driving and plow status using temporal range images generated from LiDAR data.

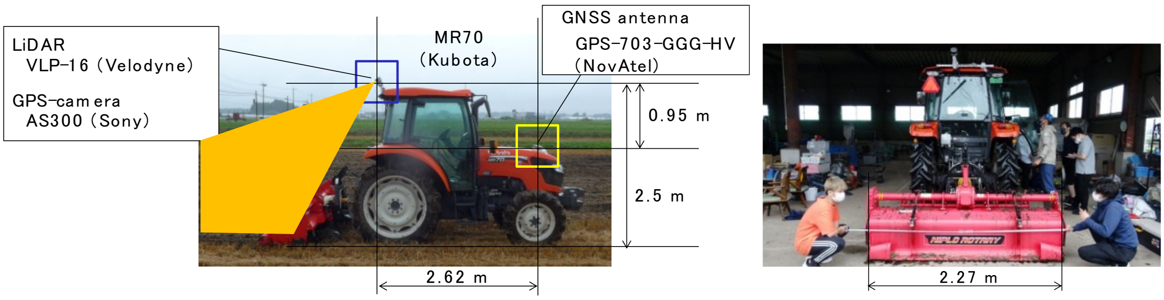


Figure 6. Measurement system

## 4. RESULTS

### 4.1 GNSS positioning

First, we have confirmed that the efficiency of positioning was improved because no preparation needs reference station installment works in SLAS, CLAS, and MADOCA. Next, we evaluated the accuracy of positioning with SLAS, CLAS, and MADOCA. RTK-GNSS positioning results were used as reference data to compare with SLAS, CLAS, and MADOCA positioning results observed during 2,200 sec in the farm area. The relative accuracy evaluation results of SLAS with the reference data are shown in Table 1, the results of CLAS with the reference data are shown in Table 2, and the results of MADOCA with the reference data are shown in Table 3. In addition, the trajectory data are shown in Figure 7.

Table 1. Relative accuracy evaluation (SLAS)

| | 3D [m] | 2D [m] | X [m] | Y [m] | Z [m] |
|---|---|---|---|---|---|
| Average | 0.5632 | 0.3122 | 0.2120 | 0.0962 | 0.3515 |
| Standard deviation | 0.2530 | 0.1348 | 0.1606 | 0.1888 | 0.3769 |
| RMSE | 0.6174 | 0.3400 | 0.2659 | 0.2119 | 0.5153 |

Table 2. Relative accuracy evaluation result (CLAS)

| | 3D [m] | 2D [m] | X [m] | Y [m] | Z [m] |
|---|---|---|---|---|---|
| Average | 0.0532 | 0.0119 | -0.0008 | -0.0020 | 0.0450 |
| Standard deviation | 0.0243 | 0.0069 | 0.0071 | 0.0116 | 0.0347 |
| RMSE | 0.0585 | 0.0138 | 0.0071 | 0.0118 | 0.0569 |

Table 3. Relative accuracy evaluation result (MADOCA)

| | 3D [m] | 2D [m] | X [m] | Y [m] | Z [m] |
|---|---|---|---|---|---|
| Average | 0.2708 | 0.2191 | -0.1972 | -0.0204 | -0.1184 |
| Standard deviation | 0.2272 | 0.1583 | 0.1547 | 0.0991 | 0.1946 |
| RMSE | 0.3534 | 0.2703 | 0.2506 | 0.1012 | 0.2277 |

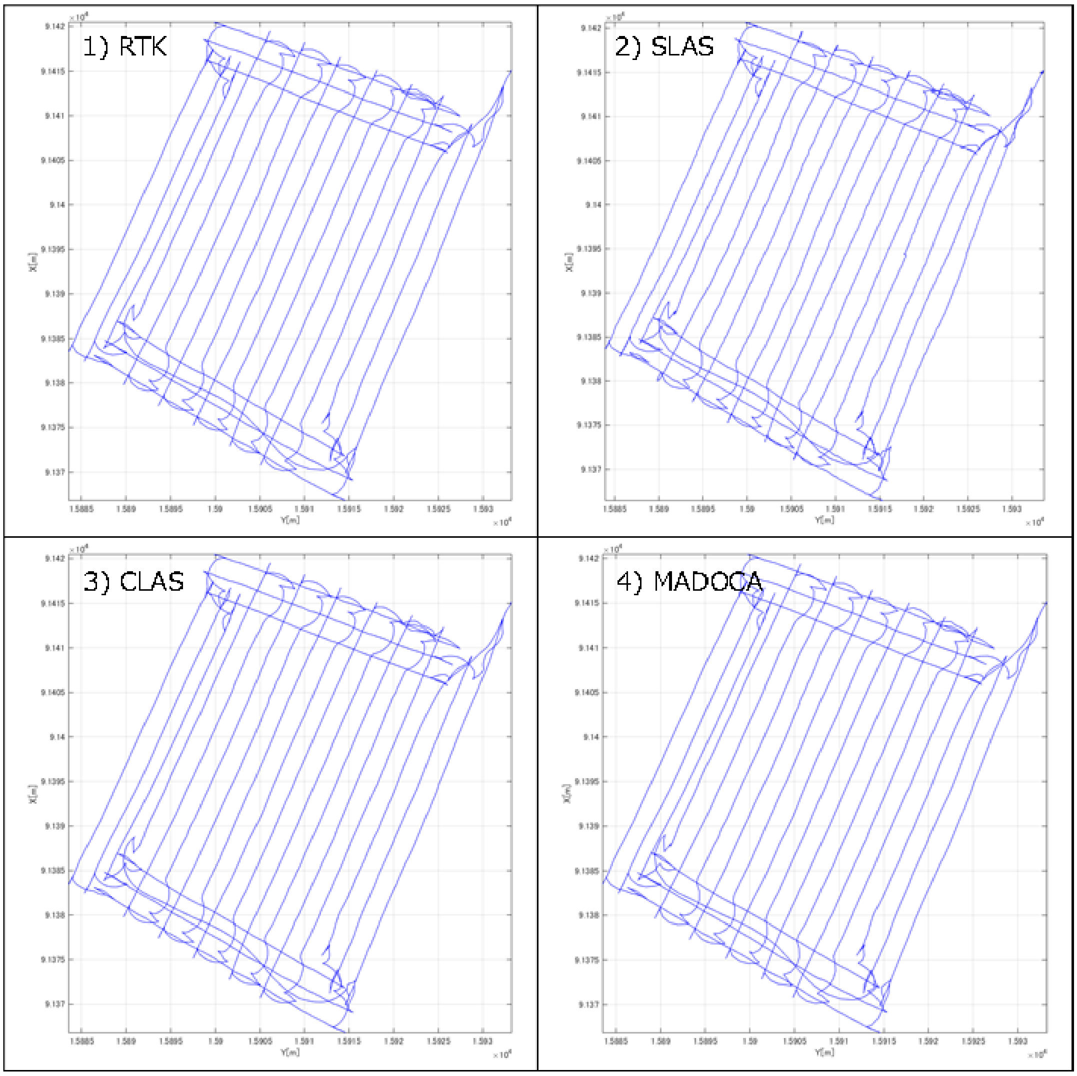


Figure 7. GNSS positioning results

### 4.2 LiDAR scan matching

We extracted the tractor's running scenes (7,132 scenes) from all scenes (22,000 scenes, 2,200 sec) in the farm area. The processing time was 7478.02 sec (Intel Core i7-10710U, 1.10 GHz), including a file import and export for 75,981,750 points. The result of scan matching was 0.0072 m (root-mean-square error [RMSE]). The integrated point clouds are shown in Figure 8. We also extracted the tractor's running scenes (500 scenes) in the road section to evaluate the versatility of methodology with the same processing environment. The result of scan matching was 0.0135 m (RMSE). The integrated point clouds are shown in Figure 9.

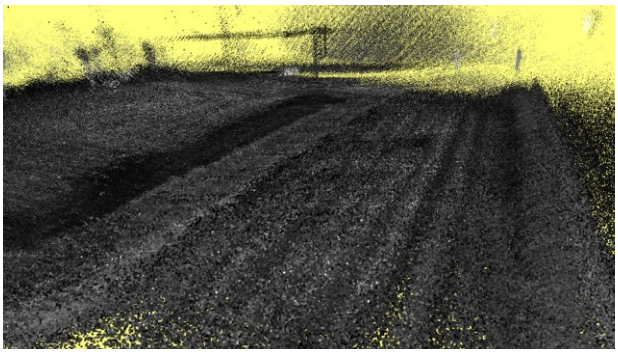

Figure 8. Integrated point clouds (farm area)

Figure 9. Integrated point clouds (road area)

### 4.3 Tractor's activity reconstruction

The tractor's activities were represented with estimated driving and plow status using temporal range images generated from LiDAR data, as shown in Figure 10. Blue points indicate LiDAR points in a scene. Red points indicate cultivated paths. Although GNSS positioning data can represent the tractor's path, cultivated areas cannot be measured. Alternatively, the result shows that precise cultivated areas can be estimated from LiDAR data used as attribute data on a base map.

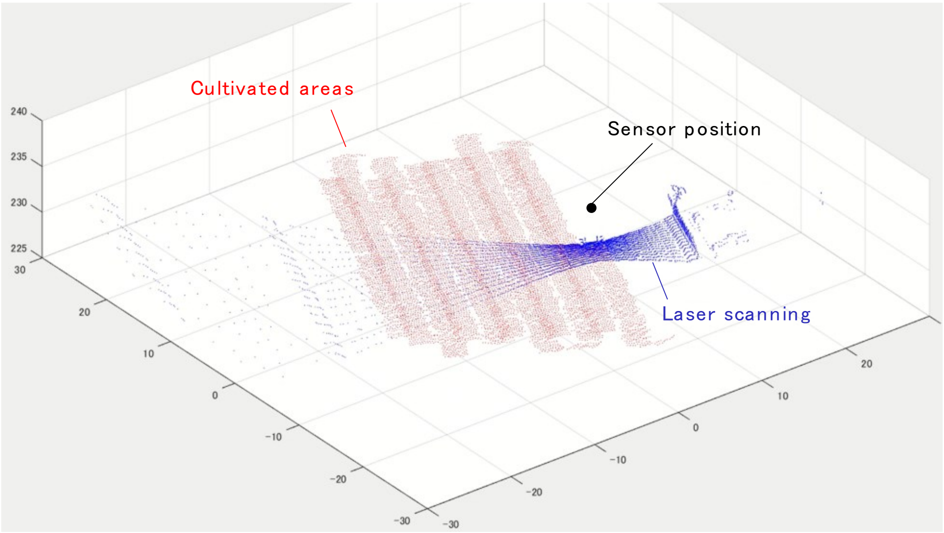


Figure 10. Tractor activity reconstruction

## 5. CONCLUSION

In this paper, we proposed a scan matching system for multilayer LiDAR data registration with RTK-GNSS positioning and geometric constraints. We selected a farm as an experiment area to acquire point clouds and position data of cultivation works before sowing soybeans and used low-price LiDAR and multifrequency GNSS devices. Through our experiment, we evaluated the positioning performance of SLAS, CLAS, and MADOCA for point cloud acquisition. Moreover, we confirmed that our methodology can reconstruct point clouds from a tractor' activities. In our future works, although we used RTK-GNSS positioning data as true values, we will conduct experiments on accuracy evaluation using ground control points and processing speed improvement for real-time processing.

### References

Friha , O., Ferrag, M., Shu., L., Maglaras, L., Wang, X., 2021. Internet of Things for the Future of Smart Agriculture: A Comprehensive Survey of Emerging Technologies, IEEE/CAA Journal of Automatica Sinica, Volume: 8, Issue: 4, pp.718-752.

Maddikunta, P., Hakak, S., Alazab, M., Bhattacharya, S., Gadekallu, T., Khan, W., Pham, Q., 2021. Unmanned Aerial Vehicles in Smart Agriculture: Applications, Requirements, and Challenges, IEEE Sensors Journal, Volume: 21, Issue: 16, pp.17608 - 17619.

Namie, H., Kubo, N., 2020. Performance Evaluation of Centimeter-Level Augmentation Positioning L6-CLAS/MADOCA at the Beginning of Official Operation of QZSS, IEEJ Journal of Industry Applications, Vol. 10 (2021), No. 1, pp. 27-35.

Nakagawa, M., Abe, S., Sanuka, S., Saito, K., Miyo, M., 2020, LiDAR Scan Matching with RTK-GNSS Positioning and Geometric Constraints, The 41st Asian Conference on Remote Sensing, 10 pages.